Effective magnetic fields near ^{238,240}Pu and ^{248}Cm nuclei in an iron matrix

A. V. Aldushchenkov and A. G. Sergeev

Leningrad Institute of Nuclear Energy, USSR Academy of Sciences
(Submitted March 12, 1976)
Zh. Eksp. Teor. Fiz. **71**, 1111–1118 (September 1976)

Hyperfine interactions of Pu and Cm in an iron matrix are investigated by applying the technique of perturbed angular correlations of α–e cascades. The atoms are introduced into an iron foil by using the recoil energy in α decay. The same technique could be used for measurements with a completely magnetized foil. In both cases the degree of suppression of the angular-correlation function is close to the "rigid-core" value ($G_2 = 0.37$). The effective magnetic fields are $B_{Pu}(Fe) = 1130 \pm 80)$ kG and $B_{Cm}(Fe) \leq 100$ kG. The magnetic field data for the actinides are discussed from the viewpoint of orbital magnetism of the $5f$-shell.

PACS numbers: 75.30.Hx

1. INTRODUCTION

The systematics of the magnetic field induced in ferromagnetic matrices on nuclei of impurity atoms point to a truly defined dependence of the magnitudes and signs of the fields on the structure of the electron shell of the impurity atom.[1,2] A characteristic singularity is possessed by magnetic hyperfine fields in rare-earth atoms imbedded in ferromagnetic matrices. The principal mechanism that ensures here the appearance of strong hyperfine magnetic fields at the nuclei is the orbital magnetism of the $4f$ shell which lies deeply in the atom.[3] As to actinides, in which the $5f$ shell is filled, the magnetic hyperfine fields are known only up to the first few elements of the actinide series. These data point to a noticable difference in the behavior of the fields in comparison with the rare-earth elements. To ascertain the mechanism whereby the fields are produced in the actinides, it is very important to investigate the hyperfine magnetic fields for the heavier elements. We have investigated the hyperfine interactions, in an iron matrix, of plutonium and curium, which lie in the middle of the actinide series.

A favorable opportunity for systematic investigations of hyperfine fields of actinides in ferromagnetic matrices is afforded by the use of the procedure of perturbed angular correlations (PAC) of the α–γ and α–e cascades. The procedure has high sensitivity, especially if the cascades 0^+–2^+–0^+, which have a large angular anisotropy, are used. The use of cascades with conversion electrons is preferred for the investigation of actinides, because the first 2^+ excited levels in these strongly deformed even–even nuclei have an energy ≈ 43 keV and the de-excitation of the levels proceeds mainly on account of internal-conversion electrons (total internal conversion coefficient $\sim 10^3$). This procedure encounters difficulties connected with the detection of soft electrons in the flux of the α particles, fission fragments, and γ quanta, and also with the deflection of the electrons in the stray field of the electromagnet, which magnetizes the iron foil. In the present study we have used a procedure that made it possible to overcome these difficulties.

2. EXPERIMENTAL PROCEDURE

We have investigated the effective magnetic fields acting on the nuclei of the Pu and Cm atoms imbedded in iron by the method of integral perturbed angular correlations.[4] We used the cascades 0^+–2^+–0^+ excited in the decays ^{242}Cm $\xrightarrow{\alpha}$ ^{238}Pu, ^{244}Cm $\xrightarrow{\alpha}$ ^{240}Pu and ^{252}Cf $\xrightarrow{\alpha}$ ^{248}Cm. Data on the energies of the 2^+ levels, on their lifetimes, the energies of the conversion electrons, the internal-conversion coefficients (ICC) of the $2^+ \to 0^+$ transitions and the anisotropy coefficients A_{22} and A_{44} are listed in Table I.

The Pu and Cm atoms were introduced into the iron foil by the recoil of α-decay, with a recoil energy ~ 100 keV. The geometry of the experiment was such that as a result of the registration of the α–e coincidences there were selected those nuclei which experienced recoil into the iron foils in the decay. Since the range of the recoil nuclei in iron is ≈ 10 μg/cm^2, the thickness of the source deposited on the foil must satisfy stringent requirements in such experiments. The thickness of the active layers in the Cm and Cr sources did not exceed 1 μg/cm^2 at an activity 5–20 μCi. The Cm source contained two isotopes, ^{242}Cm and ^{244}Cm, with an activity ratio on the order of 1 : 2. The decay schemes of the two isotopes and the lifetimes of the 2^+ levels are practically the same, so that we measured the joint effects of the two isotopes.

The magnetic moments of the 2^+ levels of the investigated nuclei were not determined. However, for strongly deformed nuclei, in analogy with rare-earth nuclei, the gyromagnetic ratio of the first excited level of rotational band is customarily assumed to be $g(2^+) = 0.3$.

TABLE I. Characteristics of the employed cascade 0^+–2^+–0^+.

Decay	$E(2^+)$	$T_{1/2}(2^+)$, nsec [5]	Shell	E_e	ICC [6]	A_{22} [7]	A_{44} [7]
^{242}Cm → ^{238}Pu	44.1	177(5)	L	23.9	580	0.96	0.18
			M	39.0	160	0.92	0.03
^{244}Cm → ^{240}Pu	42.8	164(5)	L	22.5	650	0.96	0.18
			M	37.8	185	0.93	0.04
^{252}Cf → ^{248}Cm	43.4	126(10)	L	22.0	610	0.96	0.18
			M	38.0	205	0.92	0.05

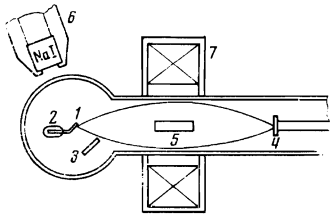

FIG. 1. Diagram of experimental setup: 1—iron-foil source, 2—electromagnet winding, 3—detector, 4—Si(Li) conversion-electron detector, 5—lead shield against fragments, α particles, and γ quanta, 6—scintillation γ detector, 7—coil of short magnetic lens.

In our experiments we used for the most part M conversion electrons, since they have a higher energy and they are less affected by the external magnetic field of the electromagnets used to magnetize the foil. In this case A_{44} is small and in the reduction of the experimental data the corresponding term in the function of the angular correlation can be neglected.

The experimental setup is shown in Fig. 1. The iron foil with the source was secured in the gap of a miniature electromagnet that magnetized the foil in a direction perpendicular to the detector plane. To register the α particles we used a surface-barrier detector, which could be rotated about the vertical axis of the vacuum chamber. The conversion electrons were recorded with an Si(Li) detector placed at the focus of a short magnetic lens with low dispersion. The lens turned out to be necessary to remove large background and the overloading of the electronic channel by fission fragments, α particles, and γ quanta of the source. To register the α–e coincidences we used a fast-slow coincidence circuit. The setup is described in greater detail.[8]

When using charged particles in the PAC procedure it is necessary to take into account the effects exerted on the particle trajectories by the stray field of the electromagnet that magnetizes the foil. The deflection of the particles in the magnetic field leads to an additional shift of the function of the angular correlation, and this can noticeably distort the experimental results. To decrease the effects, the work is carried out by using the hysteresis cycle of the residual field of the foil.[9] In this procedure, besides the small correction for the deflection of the electrons in the residual magnetic field, it is necessary to introduce a correction for the incomplete magnetization of the foil. This correction is obtained experimentally with the aid of a source that makes possible measurements with α–γ or γ–γ cascades. This procedure was used in our earlier study[8] in an attempt to determine the field at the Cm nucleus in iron. The small shift observed by us in the angular-correlation function ($\approx 2°$) turned out to be within the limits or errors, equal to the effect of the deflection of the electrons in the residual field. For the internal field at the ^{248}Cm nucleus in iron we obtained

$$B_{Cm}(Fe) \leqslant 100 \text{ kG}.$$

When working with a ^{242,244}Cm source we tested out an improved procedure, in which there is no need to determine the degree of magnetization of the foil with the aid of another sample; the entire experiment was carried out with a single sample. This procedure makes it possible to carry out the work with a fully magnetized foil. The influence of the stray magnetic field was taken into account by plotting the dependence of the shift of the angular correlation function against the external magnetic field B that magnetizes the foil fully, followed by extrapolation of this plot to $B=0$.

Figure 2 shows the experimental plot of the shift

$$R_{\theta=45°} = 2\frac{N_\downarrow - N_\uparrow}{N_\downarrow + N_\uparrow}$$

($N_\uparrow$ and $N_\downarrow$ are the numbers of the coincidences at the two different directions of the foil-magnetizing field) against the field in the electromagnet gap, obtained at room temperature of the source. In the case of the decay ^{242,244}Cm → ^{238,240}Pu, the change of R in the region $B=0$–50 G was determined by the foil magnetization curve (see the dashed curve in Fig. 2). Starting with $B=50$ G, the change of R was determined only by the deflection of the electrons in the external magnetic field. At small deflection angles ($\Delta\theta < 15°$) this part of the dependence could be approximated by a straight line. Extrapolation of the line to $B=0$ yields $R_{B=0}=R_L$—the angular-correlation-function shift connected only with the Larmor precession of the nuclear spin in the internal field B_i. This shift turned out to be opposite in sign to the shift due to the external field (see Fig. 2); it follows directly from this that the sign of the internal magnetic field at the Pu nuclei is positive. From the experimental dependence shown in Fig. 2 we determine all the sought parameters of the perturbation of the angular correlation. By way of control, the angular-correlation function was measured in the usual manner for two directions of the magnetic field at $B=50$ G (Fig. 3). These curves were corrected for the shift due to the deflection of the electrons in the external field (the $N_\uparrow$ and $N_\downarrow$ curves are moved apart in such a way that $R_{\theta=45°} = R_{B=0}$).

An analysis of the data was carried out by using the Abragam–Pound theory,[4] which takes into account the action of the transverse magnetic field on the nucleus and the presence of perturbation by dynamic electromagnetic fields:

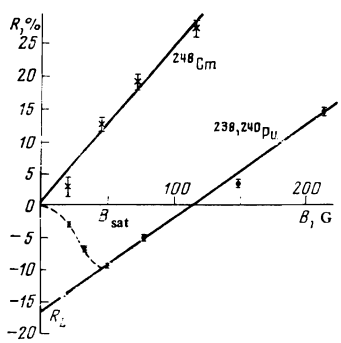

FIG. 2. Dependence of the shift $R=2(N_\downarrow - N_\uparrow)/(N_\downarrow + N_\uparrow)$ on the shield in the electromagnet gap.

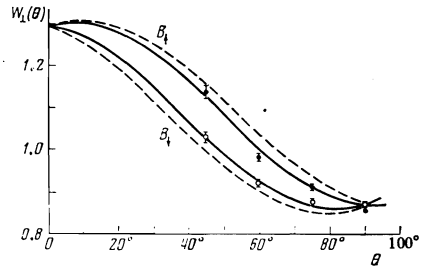

FIG. 3. Angular correlation function of α—e cascade in Pu with opposite directions of the magnetic field. The dashed curves show the same functions but corrected for the stray magnetic field.

$$W_\perp(\theta)=1+\frac{3A_{22}G_{22}}{4+A_{22}G_{22}}\frac{\cos 2[\theta+\Delta\theta+\Delta\theta_L]}{[1+(2\omega_L\tau G_{22})^2]^{1/2}}, \quad (1)$$

$$R_{\theta=45^\circ}=2\frac{W_\perp(45^\circ)-W_\parallel(45^\circ)}{W_\perp(45^\circ)+W_\parallel(45^\circ)}=\frac{6A_{22}G_{22}}{4+A_{22}G_{22}}\frac{\sin 2(\Delta\theta+\Delta\theta_L)}{[1+(2\omega_L\tau G_{22})^2]^{1/2}}, \quad (2)$$

$$\operatorname{tg} 2\Delta\theta_L=2G_{22}\omega_L\tau, \quad \omega_L=-g\mu_N B_i/\hbar, \quad (3)$$

where G_{22} is the angular-correlation-suppression factor, ω_L is the frequency of the Larmor precession in the internal field, τ is the average lifetime of the 2^+ level, and $\Delta\theta$ is an angle that takes into account the deflection of the electrons in the external field. At small deflection angles we have

$$\Delta\theta=\int B_i\,dl/B\rho\approx\alpha B.$$

where $B\rho$ is the magnetic rigidity of the electrons. It is seen from (2) that at small angles $\Delta\theta+\Delta\theta_L$ the quantity R is a linear function of B.

The experimental data were reduced by least squares using formulas (2) and (1), and the obtained angular-correlation perturbation parameters turned out to be the same, within the limits of errors, for both methods, the average values being given by $G_{22}=0.42\pm0.02$, $\omega_L\tau=-(0.41\pm0.03)$ rad. At $g(2^+)=0.3$ we have $B_i=B_{Pu}(Fe)=(1130\pm80)$ kG.

Similar experiments were performed with a ^{252}Cf source. It is seen from Fig. 3 that in this case $R_{B=0}\approx0$, which corresponds to the case of absence of a noticeable field at the ^{248}Cm nuclei in iron and agrees with the data obtained by us by using the procedure of residual magnetization of the foil.[8]

Attention is called to the strong suppression of the angular correlation, both in the case of $^{238,240}Pu$ and ^{248}Cm (for ^{248}Cm we have $G_{22}=0.37\pm0.06$). To determine the possible causes of this suppression we have performed experiments in which the source was cooled to nitrogen temperatures. No noticeable temperature dependence of the suppression of the angular correlation was observed for ^{248}Cm.[8] Nor did such a dependence appear in the case of $^{238,240}Pu$: at $T=100$ °K we obtained $G_{22}=0.35\pm0.04$ and $B_{Pu}(Fe)=(1200\pm200)$ kG. The absence of a noticeable temperature dependence of the suppression factors of the angular correlation indicates that the suppression is due to a considerable degree to quadrupole interaction with the randomly oriented electric-field gradients. Our data (Figs. 2 and 3) should have therefore been reduced with allowance for the quadrupole suppression.[4] In our case such an analysis turned out to be difficult to perform because of the proximity of the observed suppression to the "rigid core" case $G_{22}=0.37$.

It should be noted, however, that just as in the case of the Abragam–Pound theory, inclusion of the quadrupole interaction leads to a strong decrease of the angle shift $\Delta\theta_L$ in comparison with the angle of rotation $\omega_L\tau$ due only to the Larmor precession.

3. DISCUSSION

Thus, for the effective magnetic fields acting on the nuclei of the atoms Pu and Cm, introduced into the iron matrix, we have obtained the following values:

$$B_{Pu}(Fe)=(1130\pm80)\ \text{kG}, \quad B_{Cm}(Fe)\leqslant100\ \text{kG}$$

under the condition that $g(2^+)=0.3$ and that the reduction of the experimental data was carried out by using the Abragam–Pound theory. We were the first to measure the field for Cm in iron. In[10], a value $B_{Cm}(Ni)\leqslant50$ kG was obtained for the magnetic field at the ^{245}Cm in nickel from the value of the suppression of the angular correlation of the $\alpha-\gamma$ cascade. As to the field at Pu, it was determined in[11] by the method of the PAC of the $\gamma-e$ cascade $2^+-2^+-0^+$ in the $^{238}Np\xrightarrow{\beta}{}^{238}Pu$ decay; the value obtained was $B_{Pu}(Fe)=(620\pm120)$ G. The field in that reference is patently underestimated, since the authors did not take into account the suppression of the angular correlation.

To determine the nature of the magnetic field in the actinides, it is meaningful to compare the data on the actinides and lanthanides, which have atomic shells of similar structure. Such a comparison is shown in Fig. 4. At the present time in the actinide region, we know the magnetic fields for Th, U, Pu, and Cm in iron and for Np and Cm in nickel. The field for Np in iron can be estimated by using the experimentally established fact that the magnetic fields in the impurity atoms are approximately proportional to the magnetic moments of the lattice atoms.[3] This yields $B_{Np}(Fe)\approx700$ kG.

The hyperfine magnetic fields in the lanthanide atoms are determined almost entirely by the orbital magnetism

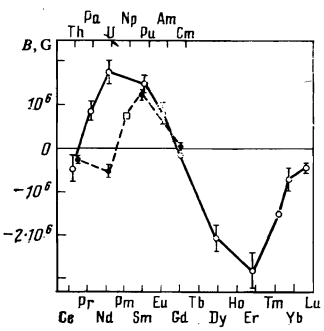

FIG. 4. Comparison of the effective magnetic fields in an iron matrix for lanthanides (solid curve) and actinides (dashed). The small square marks the value of the field for neptunium, recalculated from the known value of the field in nickel.

of the strongly localized electron $4f$ shell. The coupling between the electrons in these atoms is close to the LS type, wherein the orbital and spin moments of the atoms are oriented in the ground state antiparallel in the first half of the $4f$ shell and parallel in the second half. The exchange interaction of the impurity atoms with the iron lattice leads to an alignment of the spin momentum S, meaning also the orbital momentum L, along the direction of the foil magnetization, and it is this which produces at the nuclei a magnetic field oriented relative to this direction, the sign of the field being reversed at the midpoint of the $4f$ shell. The trivalent ion Gd^{+3} has a half-filled shell with electron configuration $4f^7$, described by the term $^8S_{7/2}$, which does not produce a magnetic hyperfine field connected with the orbital angular momentum ($L=0$). The weak field observed for Gd in iron is due to the polarization of the atomic core. The magnetic fields at the lanthanide nuclei are noticeably weaker than the hyperfine magnetic field in the free atoms, owing to the comparatively small exchange-interaction energy ≈ 0.15 eV.[12]

The data available for actinides point to a noticeable difference in the behavior of the fields—the increase of the fields in the actinide series proceeds with a delay relative to the lanthanides (Fig. 4). The field at the U nucleus is negative, whereas Nd has a large positive field. In the central part of both series, however, a similarity is observed.

The difference observed for the light actinides can be attributed to the difference between many of the properties of these actinides from the properties of the heavier actinides, and also from the properties of the lanthanides. It is known that in the initial section of the actinide series the $5f$ shell extends over a large region, and the binding energy of the $5f$ electrons are close to the binding energies of the $6d$, $7s$, and $7p$ electrons.[13] As a result, a competition in the filling of the different shells is observed for these atoms, and the $5f$ electrons participate in the formation of the chemical bonds together with the $6d$, $7s$, and $7p$ electrons. These actinides have a large variety of valences, the principal valences of Th, Pa, and U being 4, 5, and 6, respectively[14]; these elements are close in their properties to the transition $5d$ elements Hf, Ta, and W.

The trivalent state, which is the ground state for all the lanthanides, becomes the ground state for the actinides only starting with Am. With increasing atomic number the $5f$ shell becomes compressed, the binding energy of the $5f$ electrons increases, and the similarity with the corresponding lanthanides becomes more complete. Zachariassen[15] has analyzed the data on the "metallic" radii of the actinides and has reached the conclusion that there are no $5f$ electrons in metallic Th, Pa, U, and Np, and that these electrons appear starting with Pu. Dunlap and Lander[16] have shown that in intermetallic Np compounds the $5f$ electrons are strongly localized. Thus, the observed retardation in the growth of the magnetic fields in actinides can be attributed to the delay in the filling of the $5f$ shell in the initial part of the series of the actinides imbedded in iron. It appears that the negative field in U atoms is due to the $6d$ orbitals; all the transition d elements ($3d$, $4d$, $5d$) in ferromagnets have negative fields at the nuclei.[1]

In the middle part of the actinide and lanthanide series, a similarity is observed in the behavior of the magnetic fields (Fig. 4). It is known that in actinide atoms the spin-orbit interaction is much stronger than in lanthanides, and the LS coupling scheme is not as effective. Nonetheless, the principal components of the wave functions of the electron configurations $5f^n$, as shown by experiment, are described by the same terms as the analogous $4f^n$ configurations.[17,18] It is therefore reasonable to assume that the mechanism of formation of the fields in the central part of the actinide series is the same as for the lanthanides, i.e., the main contribution to the hyperfine magnetic field is made by the orbital magnetism of the strongly localized $5f$ shell. The absence of a noticeable magnetic field at the Cm nuclei can serve as an indication that the electron configuration of the Cm atom in iron is $5f^7$ with a term $^8S_{7/2}$.

When the atoms enter into the iron lattice, the recoil that takes place in the α decay causes strong disturbances in the crystal lattice; during the lifetime of the nucleus in the intermediate state, the lattice recovers only partly.[19] The impurity atoms turned out to be in this case localized in different manners: some of the atoms are located in regular sites of the lattice, and some in the interstices, and some are connected with various defects. This may make the fields at different nuclei quite different. Experiments with rare-earth atoms imbedded in an iron matrix have shown[19] that approximately half the atoms are located in regular lattice sites and the magnetic fields at their nuclei are oriented along the polarization of the lattice. The remaining atoms become interstitial and the magnetic fields in them are directed randomly; these atoms make no contribution to the integral shift of the angular-correlation function. Therefore our measurements performed by the method of the integral PAC yield a certain average field, which may turn out to be noticeably lower than the true hyperfine magnetic field in the atoms located at the regular lattice sites.

The experimentally observed strong suppression of the angular correlation is apparently connected with the randomly directed quadrupole interactions due to the crystal-lattice effects. In[20] they proved the presence of quadrupole suppression for the nuclei ^{220}Rn and ^{224}Ra in iron. If the observed suppression in the case of Pu and Cm is attributed entirely to the quadrupole interaction, then it turns out to be much stronger than in the case of Rn and Ra; this circumstance can be explained by the fact that the nuclei Pu and Cm have quadrupole moments that are approximately three times larger than the nuclei Rn and Ra.

We thank D. M. Kaminker for useful discussions and support and P. M. Levchenko for ensuring operation of the apparatus. The authors are also grateful to B. A. Aleksandrov and A. S. Krivokhatskiĭ for preparing the sources.

[1] T. A. Koster and D. A. Shirley, Preprint UCRL-20411, 1970.

[2]M. B. Stearns, Phys. Rev. [B] 8, 4383 (1973).
[3]D. A. Shirley, S. S. Rosenblum, and E. Matthias, Phys. Rev. 170, 383 (1968).
[4]R. H. Steffen and H. Fraunfelder, Perturbed Angular Correlations (Russ. transl.) Atomizdat, 1966, p. 27.
[5]É. E. Berlovich, S. S. Vasilenko, and Yu. N. Novikov, Vremena zhizni vozbuzhdennykh sostoyaniĭ atomnykh yader (Lifetimes of Excited States of Atomic Nuclei), Nauka, 1972, p. 203.
[6]R. S. Hager and E. C. Seltzer, Nucl. Data A-4, 1 (1968).
[7]R. S. Hager and E. C. Seltzer, *ibid.*, 397.
[8]A. V. Allushchenkov, A. G. Sergeev, and D. V. Yur'ev, Preprint LIYaF Akad. Nauk SSSR, No. 156, 1975.
[9]B. I. Deutsch, Proc. R. Soc. A 311, 151 (1969).
[10]F. Falk, A. Linnfors, B. Orre, and J. Thun, Phys. Scripta 1, 13 (1970).
[11]H. Ravn, F. Abildskov, H. K. Johansen, and B. I. Deutch, Proc. Nashville Conf., 1969.
[12]H. Bernas and H. Gabriel, Phys. Rev. B7, 468 (1973).
[13]J. J. Katz and G. T. Seaborg, Chemistry of the Actinide Elements, Methuen, 1957 (Russ. transl., Atomizdat, 1960, p. 514.
[14]V. I. Spitsyn, Radiokhimiya 16, 659 (1974).
[15]W. H. Zachariassen, J. Inorg. Nucl. Chem. 35, 3487 (1973).
[16]B. D. Dunlap and G. H. Lander, Phys. Rev. Lett. 33, 3487 (1973).
[17]A. Abragam and B. Bleaney, Electron Paramagnetic Resonance of Transition Metals, Oxford, 1970.
[18]A. I. Soinski and D. A. Shirley, Phys. Rev. C10, 1488 (1974).
[19]H. de Waard, Phys. Scripta 11, 157 (1975).
[20]F. Abildskov, E. I. Ansaldo, B. I. Deutch, G. M. Heestand, H. Ravn, and A. G. Sergeev, Nucl. Phys. A194, 292 (1972).

Translated by J. G. Adashko

X-ray *K*-line shifts in metallic europium and samarium in the 77–1000 K range

A. E. Sovestnov, A. S. Ryl'nikov, O. I. Sumbaev, and V. A. Shaburov

B. P. Konstantinov Institute for Nuclear Physics of the Academy of Sciences of the USSR, Leningrad
(Submitted February 18, 1976)
Zh. Eksp. Teor. Fiz. **71**, 1119–1121 (September 1976)

The shifts in the x-ray K lines of metallic Eu and Sm have been measured in the following phase transition regions: the antiferromagnetic–paramagnetic transition, the structural transition αSm→hcp, and the transition involving λ-anomaly in the heat capacity. The size of the shifts permits one to conclude that none of these transitions is associated with a change of more than 0.07 electron/atom in the number of $4f$ electrons.

PACS numbers: 32.10.Fn, 64.70.Kb, 32.10.Nw, 75.30.La

Phase transitions accompanied by anomalies in thermodynamic, magnetic, and electrical properties are observed in metallic Eu at $T_1 = 86$ K and $T_2 = 756$ K,[1] and Sm at $T_1' = 106$ K, $T_2' = 696$ K, and $T_3' = 835$ K.[2] At the low temperatures (T_1 and T_1') these are antiferromagnetic–paramagnetic transitions; the transition at $T_3' = 835$ K in samarium has been attributed with the αSm → h.c.p. structural transition[2]; the nature of the transitions at T_2 and T_2', accompanied by λ-anomalies in the heat capacity, has not been hitherto established so unambiguously. It is thought that the latter may be due to a rearrangement of the electronic structure of the metals e.g., thermal excitation of $4f$ electrons into the conduction band.[2,3]

The nature of phase transitions in the rare-earth elements involving transfer of a $4f$-electron to the conduction band can be very conveniently investigated by studying displacements in the x-ray K lines.[1)] We have previously used this method in studies of isomorphous transitions in metallic Ce and SmS[4,5]; it has also been used in investigating $Gd_xSm_{1-x}S$, $Nd_xSm_{1-x}S$, and $Nd_xSm_{1-x}Se$.[6] In the present work an experimental determination was made of the shifts in the K_{β_1} lines of metallic Eu and Sm as a function of the temperature of the samples. The measurements were carried out by the procedure described earlier[4]; in the case of the high-temperature experiments ($T > 300$ K) the samples, in the form of foils ($20 \times 20 \times 0.2$ mm, purity according to data from the manufacturing factory 99.9%), were placed in quartz ampoules filled with argon and provided with an external heater. The temperature of the sample was determined by the heater current which was calibrated from the melting points of Sn, Zn, and Eu. The relative error in determining the temperature of a sample did not exceed 4%. The absence of oxidation and of irreversible changes in the specimens resulting from the high-temperature experiments was confirmed by checks on the shifts in the x-ray lines after the samples had returned to room temperature.

Figure 1 shows the variation in the K_{β_1}-line shifts of Eu and Sm with temperature (the shifts were measured against identical samples at room temperature). The analogous variations in the heat capacities $C(T)$ of these metals obtained in other work[1,2,7] are reproduced in the upper part of the figure. Within the limits of measurement errors the K_{β_1}-line shifts of Eu and Sm were close to zero at all the temperatures investigated. Since the K_{β_1}-line shifts upon total removal of a $4f$-electron from